Heralded phase-contrast imaging using an orbital angular momentum phase-filter

2016 J. Opt. 18 055204

(http://iopscience.iop.org/2040-8986/18/5/055204)

OPEN ACCESS
IOP Publishing
Journal of Optics
J. Opt. 18 (2016) 055204 (5pp)
doi:10.1088/2040-8978/18/5/055204

Heralded phase-contrast imaging using an orbital angular momentum phase-filter

Reuben S Aspden[1], Peter A Morris[1], Ruiqing He[2], Qian Chen[2] and Miles J Padgett[1]

[1] School of Physics and Astronomy, University of Glasgow, Glasgow, G12 8QQ, UK
[2] School of Electronic and Optical Engineering, Nanjing University of Science and Technology, Nanjing 210094, People's Republic of China

E-mail: reuben.aspden@glasgow.ac.uk

Received 30 October 2015, revised 18 February 2016
Accepted for publication 18 February 2016
Published 21 March 2016

Abstract

We utilise the position and orbital angular momentum (OAM) correlations between the signal and idler photons generated in the down-conversion process to obtain ghost images of a phase object. By using an OAM phase filter, which is non-local with respect to the object, the images exhibit isotropic edge-enhancement. This imaging technique is the first demonstration of a full-field, phase-contrast imaging system with non-local edge enhancement, and enables imaging of phase objects using significantly fewer photons than standard phase-contrast imaging techniques.

Keywords: phase-contrast imaging, orbital angular momentum, ghost imaging

(Some figures may appear in colour only in the online journal)

1. Introduction

Phase-contrast imaging is a technique widely used to enable the visualisation of phase changes within an otherwise transparent object. Phase contrast imaging was first developed by Zernike as a means of converting a change in phase in the object to a change in intensity of the resulting image, thus enabling the imaging of translucent cells in a microscope [1]. The application of different phase filters within such a microscope enables a variety of edge enhancement modalities that are observable in the intensity of the resultant images. One particularly interesting form of phase-contrast imaging, pioneered by Ritsch-Marte and co-workers, uses a spiral phase filter to give isotropic edge enhancement [2, 3]. In such a system, the spiral phase filter is inserted into a Fourier plane of the imaging system, either in the illumination or the imaging optics. These spiral phase filters are exactly the same optical element used to impart orbital angular momentum (OAM) onto a transmitted laser beam [4]. Rather than using a transmissive spiral phase plate, it is more usual to implement this spiral phase filter by using its holographic equivalent, i.e. a diffraction grating containing a fork singularity [5], see figure 2 inset.

Rather than conventional imaging, this paper reports a ghost imaging (GI) technique using correlations between the signal and idler photons produced in spontaneous parametric down-conversion (SPDC). In the first demonstration of GI [6], the sample was illuminated by the signal photons from the SPDC source and any transmitted photons were subsequently detected by a single element detector, large enough to collect light from the entire field of view. Meanwhile, a scanning detector with a much smaller active area recorded the position of the correlated idler photons from the SPDC source. The image could not be retrieved from the measurements of either of the individual detectors, however, the image information could be obtained from the coincidence detection of the signal and idler photons. The strong spatial correlations between the signal and idler photons generated by SPDC have been widely utilised in many different imaging systems [7–12], and it has since been shown that classical correlations can also be used to demonstrate similar GI effects [13–15], including phase contrast imaging [16–18], albeit with the image superimposed on a background pedestal. However, most classical GI techniques rely on partial correlations between a series of speckle patterns with the object

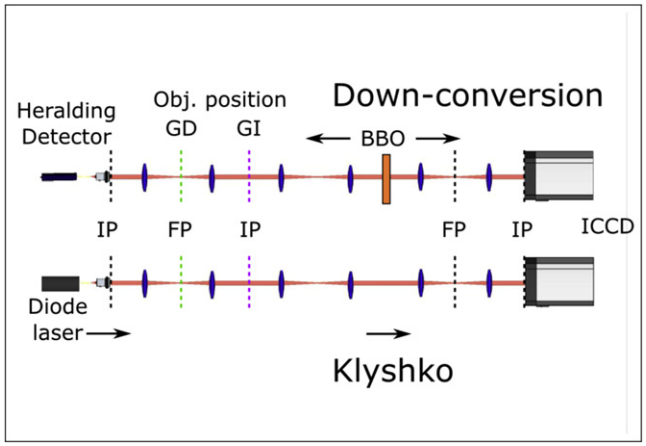

Figure 1. Top: simplified unwrapped schematic of a ghost imaging system, where the camera and the heralding detector are both in image planes of the BBO crystal. For ghost diffraction (GD) the object is placed in a Fourier-plane (FP), marked in green, whereas for ghost imaging (GI) the object is in an image plane (IP), marked in purple. Bottom: Klyshko equivalent model of the imaging system, where the heralding detector is replaced by a light source and the light is propagated back through the system to the camera. The arrows show the direction of propagation of the beams.

and so results in an image superimposed on top of a very large background pedestal, whereas the time correlation between our down-converted photons enables quantum GI to detect the near-perfectly correlated photon within a very short time window, thus removing the pedestal background.

The use of a scanning single element detector to recover the spatial information in the idler beam fundamentally limits the detection efficiency of the imaging system to a maximum of $1/N$, where N is the number of pixels in the image. Previously, we overcame this limitation by replacing the scanning detector by an intensified CCD (ICCD) camera, therefore detecting all idler photons irrespective of their position within the image. In that system the detection of the signal photon after the object by the non-imaging, single-element detector, was used to trigger the ICCD, effectively heralding the arrival of the correlated idler photon [10]. Hence, in this configuration we refer to the non-imaging, single-element detector as the 'heralding' detector.

Beyond GI it is also possible to perform ghost diffraction. In any imaging system, the detector must be in an image plane of the object. In a GI configuration the object and the imaging (or scanning) detector are commonly positioned either both in an image plane of the crystal, or both in the Fourier-plane of the crystal. This positioning of object and imaging detector can be understood within a Klyshko model of GI as corresponding to the object being imaged onto the plane of the[3] detector [19]. This equivalence between the Klyshko picture and the SPDC configuration is shown in figure 1. For ghost diffraction the object can again be placed in either the image plane or the Fourier-plane of the crystal but now the imaging detector is placed in the other plane. Within the Klyshko model this positioning corresponds to the imaging detector being placed in the Fourier-plane of the object. Beyond the considerations of the relative planes of the object and detector, the Klyshko model is a useful predictive model that fully predicts the results of GI using classical optics whether when imaging [20] or, as shown in this paper, according to the well developed theory of spiral phase-contrast imaging [24].

However, even in classical diffraction experiments, both in a standard imaging configuration or ghost configuration, this positioning of the object and camera alone does not result in a high-contrast diffraction pattern [21]. To obtain a high-contrast diffraction pattern, in addition to correct positioning, the illuminating light source needs to be spatially coherent. For ghost diffraction, this spatial coherence is not applied to the illuminating down-converted light but, inspired by the Klyshko model, is applied to the spatial selectivity of the non-imaging, single-element detector. The importance of the spatial (or spatial mode) selectivity of the non-imaging single-element detector has been studied previously [22]. In practice, if the non-imaging detector is fibre coupled, then the degree of spatial selectivity is easily controlled by choice of the coupling fibre which can be either multimodal (for a normal imaging configuration) or single mode (for ghost diffraction configuration). Similar spatial selectivity considerations apply in this present work to give a phase imaging configuration. Even in a conventional microscope, high-contrast phase imaging requires control of the spatial coherence of the illuminating light source. Therefore, within our phase-contrast GI system we restrict our non-imaging, single-element detector to a single transverse detection mode through use of a single-mode fibre. We have previously shown a phase-contrast, GI system but that system was based upon scanning the object within a single beam system and reconfiguring the time sequenced data into a 2D image [23]. By contrast, this present system images with a camera across the full field of view.

2. Methods

Our experimental setup is shown in figure 2. Spatially correlated (and OAM anti-correlated) signal and idler photons are generated by the SPDC process and are detected by two spatially separate detectors: a single-photon avalanche detector (SPAD) in the signal arm and an ICCD in the idler arm. The SPAD detects a signal photon transmitted by the object and triggers the ICCD camera to record the position of the position-correlated idler photon. The SPDC source consists of a 3 mm long, β-barium borate (BBO) crystal pumped by a horizontally polarised, quasi-continuous wave laser at 355 nm. This pump laser is spatially filtered and collimated such that the beam incident on the crystal is a 0.5 mm at full-width half-maximum (FWHM) fundamental Gaussian mode. The crystal is cut for type-I phase matching and generates colinear, frequency-degenerate signal and idler beams. These beams are separated from the pump beam by high-transmission interference filters, centred at 710 nm with a 10 nm

[3] The Klyshko, back-projection representation is where the non-imaging, single-element detector within a GI system is replaced by a light source and the nonlinear crystal by a mirror, thereby creating a classical imaging system.

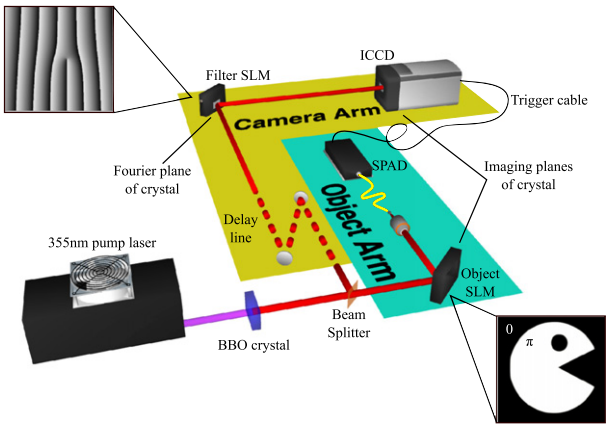

Figure 2. Experimental schematic. Twin correlated photons produced by pumping a BBO crystal were separated at a beam splitter. One photon propagating through the object arm of the system was incident upon a phase object placed in the image plane of the crystal before its subsequent detection by a SPAD. The detection pulse from the SPAD was then used to trigger the intensifier of an ICCD placed in the camera arm of the system. The photons in this arm first propagated through an optical delay line to ensure it arrived in sync with its correlated partner's electronic pulse. This photon is endowed with OAM by use of a phase filter placed in the Fourier-plane of the crystal before its spatial information is recorded by the ICCD in the image plane of the crystal. For the heralding system to correctly function it is necessary that camera and object are in similar planes of the crystal, i.e. both image plane or both Fourier-plane.

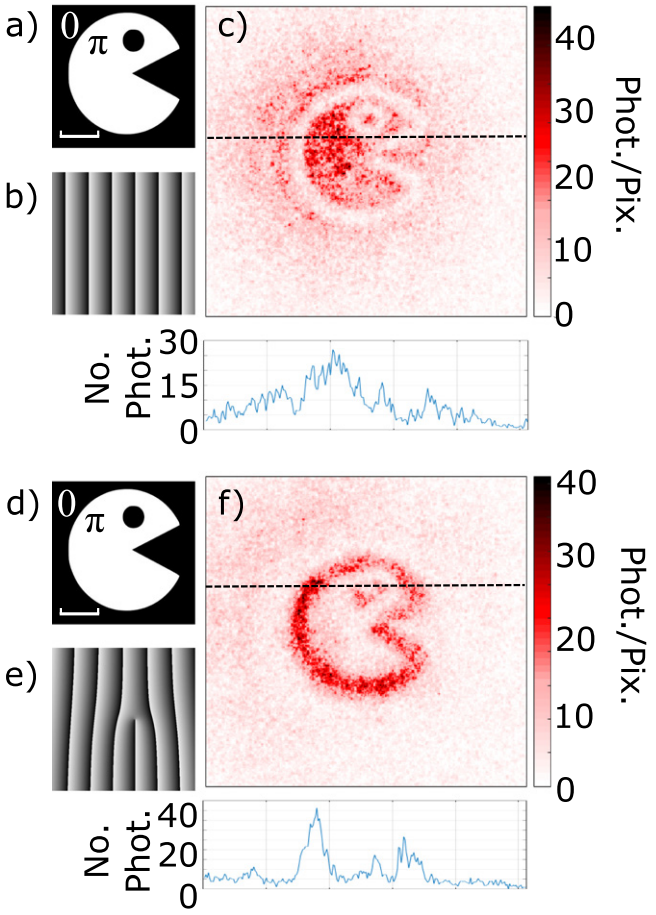

Figure 3. Results: the use of a simple blazed grating (b), in the Fourier-plane of the object (a), does not provide any phase filtering and so the lines of phase discontinuity in the object appear as a line of zero intensity in the image (c). Using a spiral phase filter (e), in the Fourier-plane of the object enhances the lines of phase discontinuity in the object (d), leading to isotropic bright lines on a dark background, shown in (f). The scalebar represents 200 μm and the cross-sections are the average of the 5 pixels centred around the dotted line.

bandwidth. The large Gaussian profile of the pump beam compared with the short length of the crystal ensures the down-converted photons exhibit strong correlations over a wide range of spatial positions [9]. The signal and idler beams are separated into the camera and object arms of the experiment using of a pelicle beam splitter placed in the Fourier plane of the crystal. Each arm has an optical magnification of $M = 3$ from the plane of the crystal to the plane of the detectors. In the object arm the crystal is re-imaged on to a spatial light modulator (SLM) (Hamamatsu), onto which we encode a phase-only object. This phase object is therefore illuminated by a spatially incoherent beam of 1.5 mm (FWHM). The photons transmitted by the object are detected by the heralding detector consisting of a 20× objective lens, a single-mode fibre and a SPAD. This heralding detector records the presence of a photon but does not measure any specific spatial position. As discussed in the previous section, the single-mode selectivity of this heralding detector is necessary in order to achieve high-contrast, phase-contrast images [22]. In the camera arm, a second SLM (the phase filter) is located in the Fourier-plane of the crystal and an ICCD camera is located in a subsequent imaging plane of the crystal. The intensifier of the camera is triggered by the output of the heralding SPAD. The CCD then records the spatial position of the correlated idler photon. A free-space, image-preserving optical delay line is included in the camera arm to compensate for the electronic delay associated with the trigger electronics of the camera, and this delay arm ensures that for each photon detected by the SPAD, only its correlated partner is recorded by the ICCD [10]. The triggering electronics of the camera allows us to set the intensifier gate width (the length of time the intensifier is active per trigger signal) at 4 ns, virtually eliminating the detection of uncorrelated photons. Additionally, the pump beam is attenuated such that there is only a very small probability of double photon-pair production per pulse of the pump laser. This scarcity of pair production ensures that the photon detected by the ICCD was from the same pair as that detected by the SPAD.

As discussed above, within a conventional microscope, even if the illumination has a high degree of spatial coherence, an object of constant phase is imaged as a uniform intensity. However, the edge of any phase object results in light being scattered/diffracted out of the numerical aperture of the collection optics and hence any phase step in the object appears as a dark line in the image. The contrast of the line depends upon the (spatial) modal selectivity of the illumination/imaging optics and the width of the dark line depends

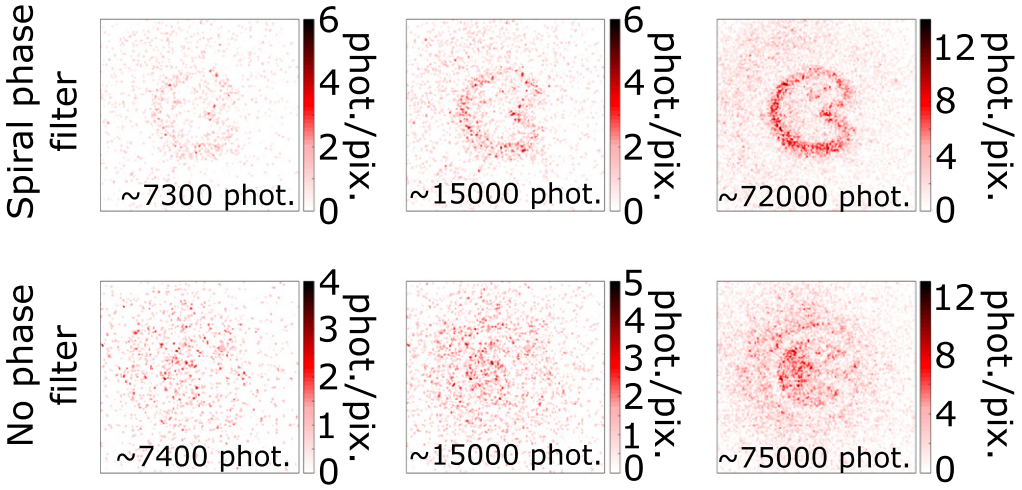

Figure 4. Images of the pacman phase object for an increasing number of photons.

upon the resolution of the imaging optics. For single-mode illumination/imaging selectivity, the observed contrast of a π-phase step can reach 100%. As mentioned in the introduction, rather than selecting the fundamental spatial mode, a spiral phase filter can be inserted into a Fourier-plane of the object [24]. As discussed, this spiral phase filter is exactly the same optical element that would be used to transform a fundamental Gaussian mode into a laser beam carrying OAM, i.e. a beam with helical phasefronts. With such a filter in place, a uniform phase object gives rise to a dark image. Any phase edge within the field of view now appears as a bright line, irrespective of its orientation. Hence, the spiral phase filter in the Fourier-plane of the phase object provides isotropic edge-enhancement of the intensity image.

In our implementation using a correlated SPDC source, the object and the phase filter are placed in different optical paths, i.e. none of the light which interacts with the object is ever processed by the phase filter. Leaving aside timing loopholes, our configuration therefore is one in which the phase-filter is non-local with respect to the object. It should be noted however that non-local correlations of this type are not in themselves proof of quantum entanglement, the latter requiring demonstrations of measurements in complimentary bases.

3. Results

Figure 3 shows two images obtained from a pacman phase-only object encoded onto a SLM placed in the object arm containing the single-mode, single-element detector, whereas the phase-filter is placed in the other arm containing the camera. The first image is obtained using a plane-wave filter whereas the second uses a spiral-phase filter. Both images are formed from the accumulation of 21 600 frames, each of 1 s during which the intensifier was triggered for each signal photon detection at the heralding detector. The trigger rate from the single-element detector was approximately 1800 times a second with a dark count rate of 1200 a second from the SPAD. As in the conventional phase-imaging case, switching between a plane-wave and a spiral-phase filter reverses the contrast of the image, the latter giving an isotropic edge enhancement. However, as discussed above, in this case the object and phase filter are non-local with respect to each other, never interacting with the same photons. The average contrast for the non-edge-enhanced image, figure 3(c), is calculated as 58% with a maximum contrast of 69%. The average contrast for figure 3(f), the edge-enhanced image is calculated as 67% with a maximum contrast in the centre of the image of 84%, where we define contrast as $C = \frac{I_{\max} - I_{\min}}{I_{\max} + I_{\min}}$. The background noise in the images arises predominantly from read-out noise from the camera and uncorrelated photons detected when the camera is triggered from dark counts from the SPAD.

For long exposure images, as shown in figure 3, the image of the pacman is clear both with and without the spiral phase filter. However, our system also allows us to obtain images using very low light levels, as shown in figure 4. The images shown contain between 7300 and 75 000 photons, as counted using the photon counting methodology described in [25]. In this method, a threshold signal is applied to each frame read out from the ICCD camera and any signal over this threshold level is counted as a photon. We then sum all the photons in the accumulated image. The heralding efficiency of our system, the probability of detecting a photon at the camera for each detection at the heralding detector, of our system was $\approx$1%, and so while the number of photons illuminating the sample is of order 200 times more than that detected in the final image, we are still using a very low-light illumination source. In this low-light regime, it is interesting to note that the use of a spiral phase filter enables the identification of a phase object approximately an order of magnitude quicker than unfiltered phase-contrast imaging. When using the spiral phase filter it is clear that there is an object after just 7300 photons detected at the ICCD, where as without the filter it is not clear until there are around 75 000 photons in the image.

From the above numbers it is clear that our system suffers from a modest detection efficiency and correspondingly long acquisition times. However, by using the high timing correlations between the photons and the high timing resolution of the ICCD camera, the camera intensifier only fires for 3.6 ms during our 500 s exposure time. Our heralding detector detects 600 photons per second, as stated above. Therefore, for a standard imaging system to develop an image containing 7300 photons would require a total exposure time of 12 s. Thus, despite our low detection efficiency, the camera in our phase-contrast GI system is active for a time window 3000 times shorter than a conventional system would require and so detects far fewer spurious noise events, thus significantly increasing the contrast in the final images.

4. Conclusion

In this paper we extend our previous work on a camera-enabled heralded imaging system (GI) to that of a phase-contrast configuration. This configuration allows us to image transparent phase objects illuminated by the signal photons, with the image exhibiting isotropic edge enhancement. We achieve this imaging capability by introducing a non-local (with respect to the object) spiral-phase filter in the Fourier plane of the camera which is positioned to record the position-correlated idler photons. Our imaging system enables the imaging of phase objects using very few photons, and the use of this phase filter in this system enables the identification of an object with the detection of just 7300 photons. This is an order of magnitude fewer photons than required when using our system in a non-edge-enhanced GI configuration, and with an active exposure time three orders of magnitude shorter than standard imaging techniques, allowing for the acquisition of high-contrast images. This reduction in exposure time virtually eliminates the camera dark noise.

Acknowledgments

This work was funded by the UK EPSRC through a Program Grant (EP/I012451/1) and the ERC through an Advanced Grant (TWISTS). Raw data can be found in open-access repository at DOI http://dx.doi.org/10.5525/gla.researchdata.273.

References

[1] Zernike F 1942 Phase contrast, a new method for the microscopic observation of transparent objects part I *Physica* **9** 686–98
[2] Furhapter S, Jesacher A, Bernet S and Ritsch-Marte M 2005 Spiral phase contrast imaging in microscopy *Opt. Express* **13** 689–94
[3] Jesacher A, Fürhapter S, Bernet S and Ritsch-Marte M 2005 Shadow effects in spiral phase contrast microscopy *Phys. Rev. Lett.* **94** 233902
[4] Beijersbergen M W, Coerwinkel R P C, Kristensen M and Woerdman J P 1994 Helical-wavefront laser beams produced with a spiral phaseplate *Opt. Commun.* **112** 321–7
[5] Bazhenov V Y, Vasnetsov M V and Soskin M S 1990 Laser-beams with screw dislocations in their wave-fronts *JETP Lett.* **52** 1037–9
[6] Pittman T B, Shih Y H, Strekalov D V and Sergienko A V 1995 Optical imaging by means of two-photon quantum entanglement *Phys. Rev.* A **52** 3429–32
[7] Fonseca E J S, Ribeiro P H S, Padua S and Monken C H 1999 Quantum interference by a nonlocal double slit *Phys. Rev.* A **60** 1530–3
[8] Gomes R M, Salles A, Toscano F, Souto Ribeiro P H and Walborn S P 2009 Observation of a nonlocal optical vortex *Phys. Rev. Lett.* **103** 033602
[9] Shapiro J H and Boyd R W 2012 The physics of ghost imaging *Quantum Inf. Process.* **11** 949–93
[10] Aspden R S, Tasca D S, Boyd R W and Padgett M J 2013 EPR-based ghost imaging using a single-photon-sensitive camera *New J. Phys.* **15** 073032
[11] Lemos G B, Borish V, Cole G D, Ramelow S, Lapkiewicz R and Zeilinger A 2014 Quantum imaging with undetected photons *Nature* **512** 409
[12] Morris P A, Aspden R S, Bell J E C, Boyd R W and Padgett M J 2015 Imaging with a small number of photons *Nat. Commun.* **6** 5913
[13] Bennink R S, Bentley S J and Boyd R W 2002 Two-photon coincidence imaging with a classical source *Phys. Rev. Lett.* **89** 113601
[14] Gatti A, Brambilla E, Bache M and Lugiato L A 2004 Ghost imaging with thermal light: comparing entanglement and classical correlation *Phys. Rev. Lett.* **93** 093602
[15] Sun B, Welsh S S, Edgar M P, Shapiro J H and Padgett M J 2012 Normalized ghost imaging *Opt. Express* **20** 16892–901
[16] Gong W and Han S 2010 Phase-retrieval ghost imaging of complex-valued objects *Phys. Rev.* A **82** 023828
[17] Shirai T, Setälä T and Friberg A T 2011 Ghost imaging of phase objects with classical incoherent light *Phys. Rev.* A **84** 041801(R)
[18] Zhang D-J, Tang Q, Wu T-F, Qiu H-C, Xu D-Q, Li H-G, Wang H-B, Xiong J and Wang K 2014 Lensless ghost imaging of a phase object with pseudo-thermal light *Appl. Phys. Lett.* **104** 121113
[19] Klyshko D N 1988 A simple method of preparing pure states of the optical-field, a realization of the Einstein, Podolsky, Rosen experiment and a demonstration of the complementarity principle *Usp. Fiz. Nauk* **154** 133–52
[20] Aspden R S, Tasca D S, Forbes A, Boyd R W and Padgett M J 2014 Experimental demonstration of Klyshko's advanced-wave picture using a coincidence-count based, camera-enabled imaging system *J. Mod. Opt.* **61** 547–51
[21] Gatti A, Bache M, Magatti D, Brambilla E, Ferri F and Lugiato L A 2006 Coherent imaging with pseudo-thermal incoherent light *J. Mod. Opt.* **53** 739–60
[22] Tasca D S, Aspden R S, Morris P A, Anderson G, Boyd R W and Padgett M J 2013 The influence of non-imaging detector design on heralded ghost-imaging and ghost-diffraction examined using a triggered ICCD camera *Opt. Express* **21** 30460–73
[23] Jack B, Leach J, Romero J, Franke-Arnold S, Ritsch-Marte M, Barnett S M and Padgett M J 2009 Holographic ghost imaging and the violation of a Bell inequality *Phys. Rev. Lett.* **103** 083602
[24] Maurer C, Jesacher A, Bernet S and Ritsch-Marte M 2011 What spatial light modulators can do for optical microscopy *Laser Photon. Rev.* **5** 81–101
[25] Tasca D S, Edgar M P, Izdebski F, Buller G S and Padgett M J 2013 Optimizing the use of detector arrays for measuring intensity correlations of photon pairs *Phys. Rev.* A **88** 013816